Colon Cancer Detection by Designing and Analytical Evaluation of a Water-Based THz Metamaterial Perfect Absorber

Zohreh Vafapour, *Member, IEEE*, William Troy, and Ali Rashidi

***Abstract*—Colon Cancer is the fourth most common form of cancer and the second-leading cause of cancer related deaths in the United States. A large part of the reason the number of fatalities is so high is late detection as when detected in the early stages of development 9 out of 10 cases of colon cancer are non-fatal 5 years after detection. Currently the main method of colon cancer detection are colonoscopies which are highly invasive and time intensive procedures. In this work we propose a new diagnostic technique for colon cancer using an InSb based device that works by a change in the spectral response of the metamaterial when exposed to electromagnetic waves in the terahertz regime and combined with cancerous colon tissue as compared to the response when combined with healthy colon tissue. We attribute this change in spectral response is due to the differing optical properties of the healthy and cancerous colon tissue as well as the creation of surface plasmon polaritons within our device.**

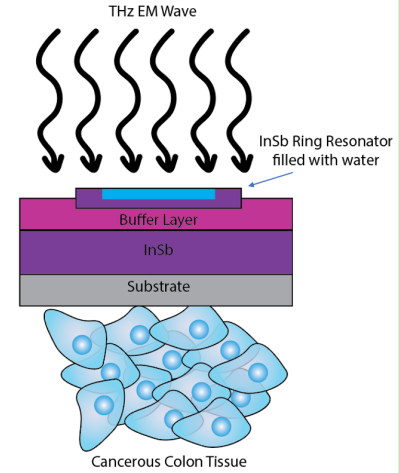

***Index Terms*— Colon cancer, cancer detection, THz metamaterials, perfect optical absorber, water-based metamaterial, semiconductor devices.**

I. Introduction

CANCER is a disease in which cells in the body grow out of control. Cells in nearly any part of the body can become cancerous and can spread to other areas of the body. When cancer starts in the colon or rectum, it is called colorectal cancer. Sometimes it is called colon cancer, for short; colon cancer and rectal cancer are often grouped together because they have many features in common. Colon cancer is one of the most common forms of cancer people experience and it is the fourth most common cancer in the United States while is the second-leading cause of cancer-related deaths in the United States. Because of the slow progress of this cancer disease, its early diagnosis has a marvelous effect on the treatment. It affects men and women of all racial and ethnic groups and is most often found in people 50 years or older. However, incidences in those younger than 50 are on the rise.

This disease takes the lives of more than 50,000 people every year. Colon cancer is highly treatable if it is discovered early. About nine out of every 10 people whose colorectal cancer is found early and treated appropriately are still alive five years later. So, the early detection process of colon cancer is vital. Some optical methods are used to detect colon cancer using infrared radiation [1], THz radiation [2], endoscopy by THz imaging [3]–[5].

THz radiation is very suitable for colon cancer detection due to non-ionization and high resolution [6]. Cancerous tissues have been shown to have higher water concentrations than that of normal, healthy, cells [7]. In this research, we exploit this property of cancerous tissue for the theoretical/numerical optical detection of colon cancer by using THz electromagnetic (EM) waves. This is possible because the absorption spectra of THz waves have been shown to be particularly sensitive to polar molecules, such as water [8]. These properties have been shown to be able to be exploited in other studies done by Woodward *et al.* [9] and Keshavarz *et al.* [10].

Besides the fact that the big advantages of THz EM waves to be sensitive to polar molecules, they are also used for

Manuscript received April 20, 2021; revised June 4, 2021; accepted June 7, 2021. Date of publication June 9, 2021; date of current version August 31, 2021. The associate editor coordinating the review of this article and approving it for publication was Dr. Yen Kheng Tan. *(Corresponding author: Zohreh Vafapour.)*

Zohreh Vafapour is with the Department of Bioengineering, and the Department of Electrical and Computer Engineering, University of Illinois at Chicago, Chicago, IL 60607 USA (e-mail: z.vafapour@gmail.com; zvafa@uic.edu).

William Troy is with the Department of Electrical and Computer Engineering, University of Illinois at Chicago, Chicago, IL 60607 USA.

Ali Rashidi is with the Department of Radiology, Molecular Imaging Program at Stanford (MIPS), Stanford University School of Medicine, Stanford, CA 94305 USA.

Digital Object Identifier 10.1109/JSEN.2021.3087953

the following reasons: They are low energy so the risk of ionization to any biological material involved is little to none. Moreover, the wavelength of EM waves in the THz regime is smaller than the size of a cell. This allows for high precision of diagnosis. Literature on the THz metamaterial has been reported using optical waveguides [11]–[14], slow light devices [15]–[18], optical buffers [19]–[21], switching [22]–[24], Optical detection [25]–[30] such as cancer [31]–[33] and virus detection [34]–[38] thermo-optical modulators [39]-[41], opto-chemical sensors [30]–[46], cloaking devices [47], [48], optical sensors [36]–[52], etc.

In the THz frequency range, semiconductors emulate metals by having negative values in the real parts of their relative permittivities. Compared to metals, nonetheless, semiconductors have a considerable improvement in that their relative permittivity can be modified by changing the temperature [10], [16], [41], external magnetic fields, pumping light intensity and applied voltages [23]. Therefore, semiconductor THz metamaterials provide one way to create tunable and switchable semiconductor devices which can be expected to be used in the valuable practical applications such as optical and biomedical sensors [10]–[12], [32], temperature sensors [16], [23], thermal modulating [16], [23], [40], [41], slow light devices [16], [17], [41], switching devices [23], chemical sensor [43], [50], etc.

Associated with metamaterial investigations and applications is the need for enabling metamaterial structures to be of utmost flexible properties. In this research, we present a state-of-the-art THz metamaterial exhibiting an optical perfect absorption feature at terahertz frequency regime (corresponding to micron wavelength regime) as well as sensing properties which has been applied in colon cancer detection but considerably consistent with theoretical analysis. In the presented THz metamaterial design, we consider incorporation of the dielectric material into semiconductor, where precise patterning of semiconductors permits frequency tuning of the metamaterial resonance by changing the external temperature. Thus, the results presented here may offer a desirable and flexible design for frequency-agile metamaterials in the THz regime and then could lead to potential applications in novel terahertz devices such as optics and photonics biomedical sensing and detecting application which is presented in the following research.

II. Materials and Methods

Figure 1 shows the engineered three-layer structure made of a semiconducting THz metamaterial thick film, a buffer layer as a dielectric spacer, and a semiconductor ring resonator antenna. The unit cell of the proposed semiconductor absorber design which is illustrated in Fig. 1 consists of a glass layer as a substrate with the thickness of 5 μm, a thick film of semiconductor layer in cross shape with size of 37 $\times$ 37 μm with the thickness of 20 μm, and a Magnesium fluoride (MgF_2) layer as a buffer. A circular hole in is then cut out of the MgF_2 buffer layer and filled with water with 8 μm thickness and radius of 27 μm as well as a semiconductor ring resonator with radius and thickness of 30 and 2 μm, respectively in the top of the structure. We used Indium

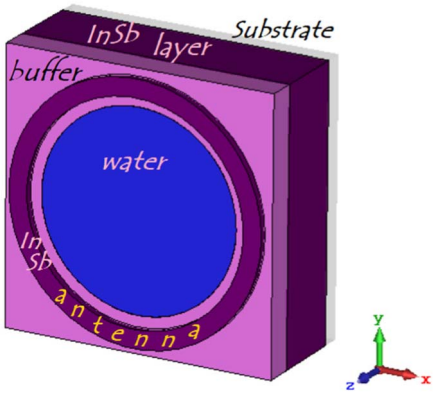

Fig. 1. The unit cell schematic of the optical absorber microstructure manufactured by CST simulator.

antimonide (InSb) as a semiconductor material in the proposed design. All materials couple to both the electric and magnetic components of the incident THz EM waves to achieve maximum of the absorbance coefficient at a specific THz frequency. The semiconductor film and dielectric buffer layer are designed to be thick enough to prevent light transmission and therefore guarantees a narrow absorption band with high absorptivity to be more appropriate for fabrication process.

Computer simulations of the spectral response of the proposed microstructure were performed using the commercial software CST Microwave Studio, which is a 3D full-wave solver that employs the three-dimensional finite difference time domain (FDTD) method. In the simulation, the metamaterial was taken to be surrounded by air and open boundary conditions were employed along the propagation direction. So that, the electric field of the normal incident THz EM waves is in x-direction and the magnetic one is along y-direction; and perfectly matched layers (PML) were applied in z-directions to eliminate non-physical boundary reflections. In the Z-direction of normal incidence, two waveguide ports are used as the excitation and collection, respectively. The open boundary conditions are employed along the propagation direction. The normal incident EM THz wave is excited from the free space, goes through the sample on the substrate, and then is collected in free space. The transmission from the whole structure is near zero, and the absorbance resonance peak is more prominent.

A. InSb Optical Parameters

Here, InSb is chosen as the semiconductor material. The Drude model describes the frequency-dependent conductivity of metals and can also be extended to free-carriers in semiconductors. In the far-infrared (Far-IR) portion of the THz frequency regime of interest, the complex-valued relative permittivity of the InSb is described by the Drude model as [16]

$$\varepsilon = \varepsilon_\infty - \frac{\omega_P^2}{\omega^2 - j\gamma\omega} \tag{1}$$

where ε_∞ represents the high-frequency value, γ is the damping constant and for InSb is calculated as $\gamma = \frac{e}{m^*\mu}$ in which μ is the electron mobility which in turn depends on temperature

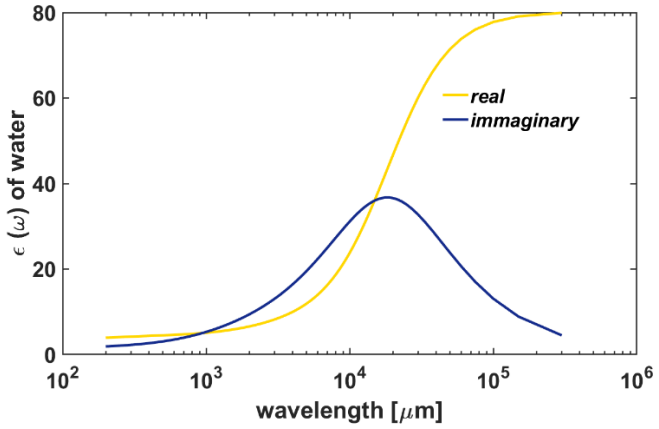

Fig. 2. The real and imaginary parts of water permittivity vs wavelength at T = 300 K.

and finally influence on the absorption of InSb microstructure. However, around 300 K within the frequency range of 0.1 to 1 THz, the electron mobility changes little [16], [32] with temperature and it is thus reasonably assumed that γ is a constant, which is consistent with the experimental report [53]. m^* is the effective mass of the free carriers and in the case of InSb is approximately $0.015m_e$, where m_e is the mass of electron. The plasma frequency, ω_P, and all related optical parameters are calculated from the relations provided in Ref. [16].

In the THz frequency range, the complex-valued relative permittivity of InSb is very sensitive to temperature [16]. Therefore, we can expect that temperature variations can cause substantial variations in the optical response characteristics of the metamaterials comprising InSb inclusions.

B. Optical Parameters of Water in THz Frequency Regime

The permittivity of water is important in that it is related to the coupling of the water with the EM field and is dependent on temperature, pressure, and field frequency. To calculate the real and imaginary parts of the water permittivity in the THz frequency regime, the three Debye model was applied as it has shown accurate in the THz regime [54]. Using the three Debye model, the total permittivity of water is given as $\varepsilon(\omega, T) = \varepsilon_{Re.}(\omega, T) + i\varepsilon_{Im.}(\omega, T)$, in which, the permittivity of water can be separated out into two different parts as a real ($\varepsilon_{Re.}$) and imaginary ($\varepsilon_{Im.}$) parts which are plotted in Fig. 2 and formulated by Eq. 2 to Eq. 4, respectively as follows:

$$\begin{aligned}\varepsilon_{Re.}(w,T) = {} & \varepsilon_s(T) - (2\pi w)^2 \\ & * \left[\frac{\Delta_1(T)\tau_1^2(T)}{1+(2\pi w\tau_1(T))^2} + \frac{\Delta_2(T)\tau_2^2(T)}{1+(2\pi w\tau_2(T))^2} \right. \\ & \left. + \frac{\Delta_3(T)\tau_3^2(T)}{1+(2\pi w\tau_3(T))^2} \right] - (2\pi\tau_4(T))^2 * \frac{\Delta_4(T)}{2} \\ & * \left[\frac{w(f_0(T)+w)}{1+\left(2\pi\tau_4(T)*(f_0(T)+w)^2\right)} \right. \\ & \left. - \frac{w(f_0(T)-w)}{1+\left(2\pi\tau_4(T)*(f_0(T)-w)^2\right)} \right] \\ & - (2\pi\tau_5(T))^2 * \frac{\Delta_5(T)}{2} \\ & * \left[\frac{w(f_1(T)+w)}{1+\left(2\pi\tau_5(T)*(f_1(T)+w)^2\right)} \right. \\ & \left. - \frac{w(f_1(T)-w)}{1+\left(2\pi\tau_5(T)*(f_1(T)-w)^2\right)} \right] \end{aligned} \quad (2)$$

And,

$$\begin{aligned}\varepsilon_{Im.}(w,T) = {} & 2\pi w \left[\frac{\Delta_1(T)\tau_1^2(T)}{1+(2\pi w\tau_1(T))^2} + \frac{\Delta_2(T)\tau_2^2(T)}{1+(2\pi w\tau_2(T))^2} \right. \\ & \left. + \frac{\Delta_3(T)\tau_3^2(T)}{1+(2\pi w\tau_3(T))^2} \right] + \pi w\tau_4(T)\Delta_4(T) \\ & * \left[\frac{1}{1+\left(2\pi\tau_4(T)*(f_0(T)+w)^2\right)} \right. \\ & \left. + \frac{1}{1\left(2\pi\tau_4(T)*(f_0(T)-w)^2\right)} \right] \\ & + \pi w\tau_5(T)\Delta_5(T) \\ & * \left[\frac{1}{1+\left(2\pi\tau_5(T)*(f_1(T)+w)^2\right)} \right. \\ & \left. + \frac{1}{1+\left(2\pi\tau_5(T)*(f_1(T)-w)^2\right)} \right] \end{aligned} \quad (3)$$

where ω is electromagnetic field frequency, T is temperature, ε_s is the static dielectric constant, τ values are relaxation times, f values are resonance frequencies, and Δ values are spectral amplitudes of the relaxing/resonating system, all calculated and given in [54]. So, the complexed-value permittivity of water can be found here:

$$\begin{aligned}\varepsilon(\omega,T) = {} & \varepsilon_s(T) + 2i\omega\pi \left[\frac{\Delta_1(T)\tau_1(T)}{1-2i\pi\omega\tau_1(T)} + \frac{\Delta_2(T)\tau_2(T)}{1-2i\pi\omega\tau_2(T)} \right. \\ & \left. + \frac{\Delta_3(T)\tau_3(T)}{1-2i\pi\omega\tau_3(T)} \right] + i\omega\pi \left[\frac{\Delta_4(T)\tau_4(T)}{1-2i\pi\tau_4(T)*(f_0+\omega)} \right. \\ & \left. - \frac{\Delta_4(T)\tau_4(T)}{1-2i\pi\tau_4(T)*(f_0-\omega)} \right] \\ & + i\omega\pi \left[\frac{\Delta_5(T)\tau_5(T)}{1-2i\pi\tau_5(T)*(f_1+\omega)} \right. \\ & \left. - \frac{\Delta_5(T)\tau_5(T)}{1-2i\pi\tau_5(T)*(f_1-\omega)} \right] \end{aligned} \quad (4)$$

From these equations, we calculate the complex-valued of the permittivity of water from 0 to 0.6 THz which are plotted in Fig. 2. These results are consistent with Keshavarz *et. al.* [10] and Ellison [54].

III. The Mechanism of Plasmon Enhancement and Creation of the Perfect Absorption

In this section of the research, we discuss the physics of absorption, the role of surface plasmon polariton, and performance of the proposed perfect metamaterial absorber.

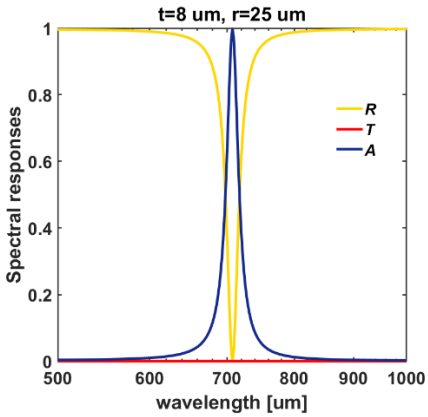

Fig. 3. Spectral responses vs wavelength.

A. Absorption Spectrum

When the incident EM THz wave is perpendicular to the surface, the absorption, $A(\omega)$ is obtained by the formula as follows:

$$A(\omega) = 1 - |S_{11}|^2 - |S_{21}|^2 \tag{5}$$

in which S_{11} and S_{21} are the Scattering parameters and calculated as follows:

$$S_{11} = \sqrt{\frac{P(R)}{P_{incident}}} \tag{6}$$

$$S_{21} = \sqrt{\frac{P(T)}{P_{incident}}} \tag{7}$$

where $P(R)$, $P(T)$, and $P_{incident}$ are the power of reflected, power of transmitted, and the total power of incident, respectively. Note that the buffer layer has a high refractive index, with semiconductor thick film thickness larger than the terahertz skin depth, there is negligible transmission through the structure with the transmission coefficient is equal to zero as

$$S_{21} \simeq 0 \tag{8}$$

Therefore, the simplified form to calculate the absorption for the proposed device is calculated as follow:

$$A(\omega) = 1 - |S_{11}|^2 \tag{9}$$

At normal incidence of THz EM wave, the spectral responses such as absorbance (A), Transmittance (T), and reflectance (R) of the proposed metamaterial absorber are illustrated in Fig. 3. It shows a negligible transmittance, highly efficient perfect absorption peaking of 99.82% at $\lambda = 707.5$ μm and a dip resonance in reflection within a wavelength range of 500 μm to 1000 μm. The optimized geometrical parameters obtained using genetic algorithm are used, together with a semiconductor at room temperature.

B. Physical Concepts: Surface Currents and Field Distributions

Surface plasmon polaritons (SPPs) are EM excitation waves that can travel along interface of semiconductor–dielectric or semiconductor–air in the THz frequency regime. The term "surface plasmon polariton" explains that the wave involves both charge motion in the semiconductor element/layer and

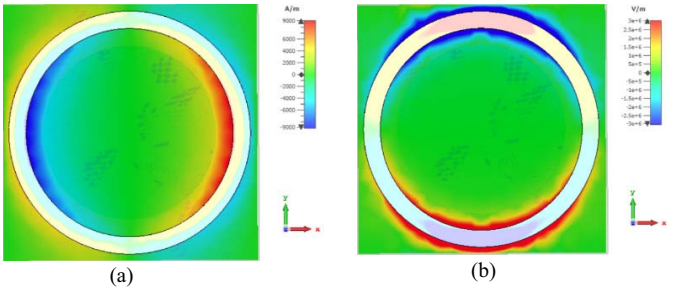

Fig. 4. The EM field distributions; (a) magnetic field, and (b) electric field distribution at wavelength of $\lambda = 707.54$ μm (corresponding to 0.424 THz).

EM waves in dielectric. SPPs are shorter in wavelength than the incident light (i.e., photons). Hence, they can have tighter spatial confinement and higher local field intensity. The SPPs have subwavelength-scale confinement perpendicular to the interface and propagate along the interface until their energy is lost either to absorption in the semiconductor element/layer or scattering into other directions, for instance into free space. Remarkable progress has been made in the field of SPPs in recent years. Control and manipulation of light using SPPs in THz frequency regime exhibit significant advantages in optics and photonics devices with very small elements. They open a promising way in areas involving optics, photonics, biology, medicine, environment, and energy, especially bio-photonics. Here, based on the physical mechanism and the peculiar properties of SPPs, we demonstrate one of the most important applications of SPPs which is used in bio-photonics. It is cancer detection.

To explore the physics underlying the creation of the perfect absorption, we show different mode EM fields including E-field and H-field, in Fig. 4a and Fig. 4b. It is found that excitation of the SPPs causing resonance peak in absorption spectrum at $\lambda = 707.54$ μm. The excitation of the first plasmonic mode occurs when the frequency of the incoming photons matches with the first localized mode of the semiconductor-dielectric-semiconductor sandwiched pattern. Therefore, a majority of photons are absorbed, and the others are reflected or transmitted through the semiconductor-dielectric-semiconductor sandwiched designed pattern. Transmitted photons are reflected back by the second semiconductor thick film layer which is called mirror layer, and some of them come out of the structure with a phase difference of π corresponding to the total distance travelled by the THz EM incident wave. This process is repeated multiple times, and these partial reflections destructively interfere with each other, leading to near zero overall reflection at the specific frequency. Alternatively, the transmission channel is closed by the semiconductor thick film, i.e., mirror layer reflector; thus, the incoming THz EM wave is completely trapped, and is finally absorbed in the proposed micro design.

IV. Application: Colon Cancer Detection

Colorectal cancer (CRC) is the third most common diagnosed and fourth most common cancer-correlated death in the world [55]. The incidence rate of the CRC has risen in the United States, specifically in the group ages of 20-49, from 8.6 to 13.1 per 100,000 between 1992 and 2016 [56].

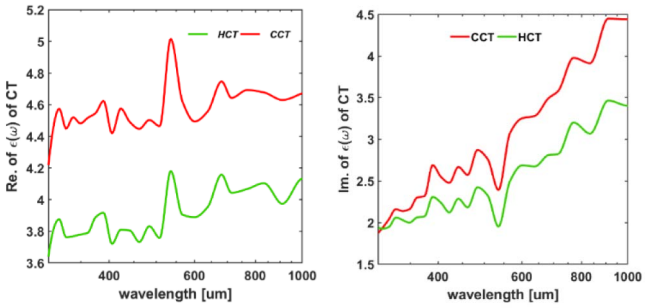

Fig. 5. The real and imaginary part of the permittivity for HCT and CCT samples vs wavelength.

Positive history of inflammatory bowel disease in individuals and personal or family history of polyp or CRC, age, obesity and alcohol or tobacco abuse, are common risk factors of CRC [57]. Most prevalent clinical presentation in CRC patients are abdominal pain, change bowel habits, hematochezia, or melena (passing blood in the stool), weakness and involuntary weight loss, anemia, peripheral edema, ascites, and palpable abdominal mass [58].

Most colorectal cancers develop first as polyps, which are abnormal growths inside the colon or rectum that may later become cancerous if not removed. While some polyps remain benignant (non-cancerous), some may become malignant (cancerous) over time. The best way to detect the presence of polyps is with a procedure called a colonoscopy, which is performed in a physician's office. For this reason, when a physician finds one or more polyps during a colonoscopy, they are generally removed during the procedure.

Early diagnosis and excision of precancerous lesion or early-stage cancers through the screening program will result in decreasing in CRC incidence and mortality. Accordingly, endoscopic techniques (flexible sigmoidoscopy, colonoscopy, and capsule colonoscopy), radiologic techniques (double-contrast barium enema and computed tomography (CT) colonography), stool testing (fecal occult blood (FOB), fecal immunochemical testing (FIT) and fecal deoxyribonucleic acid (DNA) testing), and Sept in 9 serum assays (as the first serum test for CRC screening which has been approved by FDA) are using for CRC screening [58], [59].

Optical detection is a good method to detect cancerous tissues in the THz frequency regime. Shmuel Argov *et al.* [1] proposed a diagnosis method to detect cancerous colon tissue by infrared frequency regime. Currently, THz imaging is more applicable in colon cancer imaging via an endoscope to improve endoscopic THz systems [3], [4]. Recently, Reid *et al.* [2] investigated THz imaging of colon cancer by analyzing the refractive index changes of the colon tissue samples. The dielectric constant, namely $\varepsilon(\omega)$ and the magnetic permeability, i.e., $\mu(\omega)$ are the fundamental characteristic quantities which determine the propagation of EM wave in matter. We consider magnetic permeability as a fixed amount as $\mu(\omega) \simeq 1$ because there are no significant changes in this optical parameter in comparison to this parameter in the vacuum.Here, by using their experimental optical parameters, we are analyzing the differences between absorption spectrum for different samples to detect the cancerous tissue. The

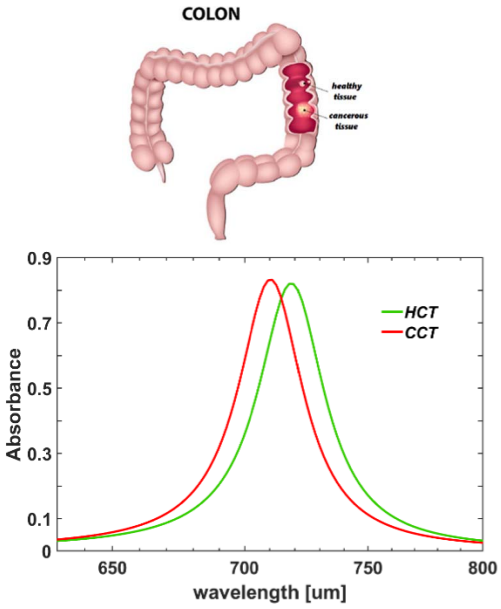

Fig. 6. The absorbance spectra vs wavelength.

electrical permittivity frequency dependent for colon tissue sample is as follow:

$$\varepsilon(\omega) = \varepsilon_r(\omega) + i\varepsilon_i(\omega) \tag{10}$$

in which, $\varepsilon_r(\omega)$, and $\varepsilon_i(\omega)$ are the real and imaginary parts of permittivity and formulated as follows:

$$\varepsilon_r(\omega) = n(\omega)^2 - \kappa(\omega)^2 \tag{11}$$

$$\varepsilon_i(\omega) = 2n(\omega).\kappa(\omega) \tag{12}$$

where κ, and n are the imaginary and real parts of the RI, respectively. The imaginary part is formulated as follows:

$$\kappa(\omega) = \frac{c \propto}{2\omega} \tag{13}$$

in which c, α and ω are speed of light in the vacuum and absorption coefficient of the sample tissues; and angular frequency which formulated as $\omega = 2\pi f$ in which f is the incident frequency of light. Figure 5 shows the real and imaginary part of the permittivity for healthy colon tissue (HCT) and cancerous colon tissue (CCT) samples.

Here, we present an optical method to differentiate between healthy colon tissues (HCT) and cancerous colon tissue (CCT) samples. Since the CCT contains more water than HCT, and the polar molecules of the water absorb THz waves more, we compare the absorption spectrum of HCT and CCT (see Fig. 6). The device is placed too close to the samples and illustrate the THz EM wave on the design. By analyzing the absorbance spectrum of the optical designed, we can identify the tissue's healthy or cancerous nature (see Fig. 6). As can be seen from Fig. 6, the CCT absorbance spectrum is blue shifted in compression with HCT sample and the maximum of the peak absorption coefficient is increased to 0.834 at $\lambda_{CCT} = 709.2$ μm (the HCT peak absorption is about 0.819 at $\lambda_{HCT} = 719.4$ μm).

We should emphasize that the proposed optical sensor which works as a colon cancer detection in the THz frequency regime can leverage additional degrees of freedom to obtain further

flexibility such as different types of semiconductors, substrate, and lattice geometry.

It is known that the proposed structure has the advantage of easy fabrication as an optical absorber. This device can be fabricated through common microfabrication techniques that are widely available. In which an overgrown InSb layer can be grown on top of a substrate layer. From there one can cut into the InSb layer through traditional photolithography and wet etching techniques to make the InSb antenna on top. The buffer layer can then be deposited on through either physical or chemical vapor deposition and the water can be added in the middle for fabrication of the device. These techniques are widely available, allowing for easy fabrication of our devices based on the schematics in this paper.

Once built these devices can then be tested by using a setup using a THz laser and monitoring the light going through the device using a THz detector on the other side of the device. Taking measurements of the light passing through the device with a healthy colon sample should provide a baseline control to be compared against when measuring light passing through cancerous colon tissue. In an experimental setup one should see results like that seen in our CST Microwave Studio model with an absorption spectrum shift in the THz regime, confirming that the tissue is cancerous.

V. Future Outlook

In this work, we present a novel device for the detection of colon cancer using terahertz electromagnetic waves by using surface plasmon polaritons within the device to detect differing water concentrations within the health colon tissue vs cancerous colon tissue. This leads to a change in the spectral response of our device, indicating that cancerous tissue is present in our sample. We believe our approach for colon cancer detection can allow for less invasive, faster, and cheaper detection of colon cancer which is pivotal in reducing the death rate of this tragic disease. Future work for this would be to build and test the device on real world samples of cancerous colon tissue and healthy colon tissue. However, CST based modeling of this problem is very promising.

Acknowledgment

The authors would like to express their special thanks to Prof. Mitra Dutta from Physics, and Electrical and Computer Engineering departments of the University of Illinois at Chicago and Prof. Michael A. Stroscio from the Departments of Bioengineering, Physics, and Electrical and Computer Engineering departments of the University of Illinois at Chicago for their useful discussions.

Funding Statement: The authors declare no conflicts of interest. There is no funding to do this research.

References

[1] S. Argov, J. Rameshm, A. Salman, I. G. J. Sinelnikov, H. Guterman, and S. Mordechai, "Diagnostic potential of Fourier-transform infrared microspectroscopy and advanced computational methods in colon cancer patients," *J. Biomed. Optic*, vol. 7, no. 2, pp. 248–255, 2020.

[2] C. B. Reid *et al.*, "Terahertz pulsed imaging of freshly excised human colonic tissues," *Phys. Med. Biol.*, vol. 56, no. 14, pp. 4333–4353, Jul. 2011.

[3] K. Wang and D. M. Mittleman, "Metal wires for terahertz wave guiding," *Nature*, vol. 432, no. 7015, pp. 376–379, Nov. 2004.

[4] Y. B. Ji, E. S. Lee, S. Kim, J. Son, and T. Jeon, "A miniaturized fiber-coupled terahertz endoscope system," *Opt. Exp.*, vol. 17, no. 19, pp. 17082–17087, 2009.

[5] P. Doradla, K. Alavi, C. S. Joseph, and R. H. Giles, "Development of terahertz endoscopic system for cancer detection," in *Terahertz, RF, Millimeter, and Submillimeter-Wave Technology and Applications IX*, vol. 9747. Bellingham, WA, USA: SPIE, 2016, Art. no. 97470F.

[6] V. P. Wallace, E. Pickwell-MacPherson, J. A. Zeitler, and C. Reid, "Three-dimensional imaging of optically opaque materials using non-ionizing terahertz radiation," *Opt. Soc. Amer. A*, vol. 25, no. 12, pp. 3120–3133, Dec. 2008.

[7] C. Yu, S. Fan, Y. Sun, and E. Pickwell-MacPherson, "The potential of terahertz imaging for cancer diagnosis: A review of investigations to date," *Quant. Imag. Med. Surg.*, vol. 2, no. 1, p. 33, 2012.

[8] M. Tonouchi, "Cutting-edge terahertz technology," *Nature Photon.*, vol. 1, no. 2, pp. 97–105, Feb. 2007.

[9] R. M. Woodward *et al.*, "Terahertz pulse imaging in reflection geometry of human skin cancer and skin tissue," *Phys. Med. Biol.*, vol. 47, no. 21, p. 3853, Oct. 2002.

[10] A. Keshavarz and Z. Vafapour, "Water-based terahertz metamaterial for skin cancer detection application," *IEEE Sensors J.*, vol. 19, no. 4, pp. 1519–1524, Feb. 2019.

[11] H. Mukundan *et al.*, "Planar optical waveguide-based biosensor for the quantitative detection of tumor markers," *Sens. Actuators B, Chem.*, vol. 138, no. 2, pp. 453–460, May 2009.

[12] L. Ali, M. U. Mohammed, M. Khan, A. H. B. Yousuf, and M. H. Chowdhury, "High-quality optical ring resonator-based biosensor for cancer detection," *IEEE Sensors J.*, vol. 20, no. 4, pp. 1867–1875, Feb. 2020.

[13] Z. Vafapour and A. Zakery, "New regime of plasmonically induced transparency," *Plasmonics*, vol. 10, no. 6, pp. 1809–1815, Dec. 2015.

[14] J. Wang and J. Dong, "Optical waveguides and integrated optical devices for medical diagnosis, health monitoring and light therapies," *Sensors*, vol. 20, no. 14, p. 3981, Jul. 2020.

[15] M. Manjappa, S.-Y. Chiam, L. Cong, A. A. Bettiol, W. Zhang, and R. Singh, "Tailoring the slow light behavior in terahertz metasurfaces," *Appl. Phys. Lett.*, vol. 106, no. 18, May 2015, Art. no. 181101.

[16] Z. Vafapour, "Slowing down light using terahertz semiconductor metamaterial for dual-band thermally tunable modulator applications," *Appl. Opt.*, vol. 57, no. 4, pp. 722–729, 2018.

[17] J. Chen, "Tunable slow light in semiconductor metamaterial in a broad terahertz regime," *J. Appl. Phys.*, vol. 107, no. 9, May 2010, Art. no. 093104.

[18] Z. Vafapour and H. Alaei, "Subwavelength micro-antenna for achieving slow light at microwave wavelengths via electromagnetically induced transparency in 2D metamaterials," *Plasmonics*, vol. 12, no. 5, pp. 1343–1352, Oct. 2017.

[19] D. Dahan and G. Eisenstein, "Tunable all optical delay via slow and fast light propagation in a Raman assisted fiber optical parametric amplifier: A route to all optical buffering," *Opt. Exp.*, vol. 13, no. 16, pp. 6234–6249, 2005.

[20] E. F. Burmeister, D. J. Blumenthal, and J. E. Bowers, "A comparison of optical buffering technologies," *Opt. Switching Netw.*, vol. 5, no. 1, pp. 10–18, 2008.

[21] Z. Vafapour, "Large group delay in a microwave metamaterial analog of electromagnetically induced reflectance," *J. Opt. Soc. Amer. A, Opt. Image Sci.*, vol. 35, no. 3, p. 417, Mar. 2018.

[22] Y. Hu *et al.*, "Bi_2Se_3-functionalized metasurfaces for ultrafast all-optical switching and efficient modulation of terahertz waves," *ACS Photon.*, vol. 8, no. 3, pp. 771–780, Mar. 2021, doi: 10.1021/acsphotonics.0c01194.

[23] Z. Vafapour, M. Dutta, and M. A. Stroscio, "Sensing, switching and modulating applications of a superconducting THz metamaterial," *IEEE Sensors J.*, early access, Apr. 13, 2021, doi: 10.1109/JSEN.2021.3073078.

[24] M. Ren *et al.*, "Nanostructured plasmonic medium for terahertz bandwidth all-optical switching," *Adv. Mater.*, vol. 23, no. 46, pp. 5540–5544, Dec. 2011.

[25] Z. Zhang *et al.*, "Sensitive detection of cancer cell apoptosis based on the non-bianisotropic metamaterials biosensors in terahertz frequency," *Opt. Mater. Exp.*, vol. 8, no. 3, pp. 659–667, 2018.

[26] Z. Geng, X. Zhang, Z. Fan, X. Lv, and H. Chen, "A route to terahertz metamaterial biosensor integrated with microfluidics for liver cancer biomarker testing in early stage," *Sci. Rep.*, vol. 7, no. 1, pp. 1–11, Dec. 2017.

[27] S. J. Park *et al.*, "Detection of microorganisms using terahertz metamaterials," *Sci. Rep.*, vol. 4, no. 1, pp. 1–7, May 2015.

[28] M. Yang *et al.*, "Electromagnetically induced transparency-like metamaterials for detection of lung cancer cells," *Opt. Exp.*, vol. 27, no. 14, pp. 19520–19529, Jul. 2019.

[29] L. La Spada, "Metasurfaces for advanced sensing and diagnostics," *Sensors*, vol. 19, no. 2, p. 355, Jan. 2019.

[30] Z. Vafapour, "Near infrared biosensor based on classical electromagnetically induced reflectance (Cl-EIR) in a planar complementary metamaterial," *Opt. Commun.*, vol. 387, pp. 1–11, Mar. 2017.

[31] D. Li *et al.*, "Identification of early-stage cervical cancer tissue using metamaterial terahertz biosensor with two resonant absorption frequencies," *IEEE J. Sel. Topics Quantum Electron.*, vol. 27, no. 4, Aug. 2021, Art. no. 8600107.

[32] Z. Vafapour, A. Keshavarz, and H. Ghahraloud, "The potential of terahertz sensing for cancer diagnosis," *Heliyon*, vol. 6, no. 12, Dec. 2020, Art. no. e05623.

[33] M. Saffarian and J. Tzeng, "Exclusive delivery of mazF in cancer cells by Listeria monocytogenes," in *Proc. Mol. Cellular Biol., Genet.*, Washington, DC, USA, Jul. 2017, p. 4314.

[34] M. Amin, O. Siddiqui, H. Abutarboush, M. Farhat, and R. Ramzan, "A THz graphene metasurface for polarization selective virus sensing," *Carbon*, vol. 176, pp. 580–591, May 2021.

[35] S. J. Park, S. H. Cha, G. A. Shin, and Y. H. Ahn, "Sensing viruses using terahertz nano-gap metamaterials," *Biomed. Opt. Exp.*, vol. 8, no. 8, pp. 3551–3558, 2017.

[36] Z. Vafapour *et al.*, "The potential of refractive index nanobiosensing using a multi-band optically tuned perfect light metamaterial absorber," *IEEE Sensors J.*, early access, Apr. 2, 2021, doi: 10.1109/JSEN.2021.3070731.

[37] D. Cheng *et al.*, "Terahertz biosensing metamaterial absorber for virus detection based on spoof surface plasmon polaritons," *Int. J. RF Microw. Comput.-Aided Eng.*, vol. 28, no. 7, Sep. 2018, Art. no. e21448.

[38] R. Jafari, Z. Esmaeilbeig, and M. Nemati, "Overcoming the bottleneck in COVID-19 detection: A machine-learning approach to improve accuracy of electrochemical impedance spectroscopy (EIS) detection sensitivity," *Open Access J. Biomed. Sci.*, vol. 3, no. 1, Oct. 2020, Art. no. OAJBS.ID.000229, doi: 10.38125/OAJBS.000229.

[39] Y. Zhou, H. Xia, L. Zhang, Y. Zhao, and W. Xie, "Temperature insensitive ultra-broadband THz metamaterial absorber based on metal square ring resonators," *Results Phys.*, vol. 22, Mar. 2021, Art. no. 103915.

[40] J. Dong and X. Zhang, "Optical modulators based on 2D materials," in *2D Materials for Photonic and Optoelectronic Applications*. Sawston, U.K.: Woodhead Publishing, 2020, ch. 2, pp. 37–77.

[41] Z. Vafapour, "Slow light modulator using semiconductor metamaterial," *Proc. SPIE*, vol. 10535, Feb. 2018, Art. no. 105352A, doi: 10.1117/12.2292259.

[42] B. Vasić and R. Gajić, "Graphene-covered photonic structures for optical chemical sensing," *Phys. Rev. A, Gen. Phys.*, vol. 4, no. 2, Aug. 2015, Art. no. 024007.

[43] M. R. Forouzeshfard, S. Ghafari, and Z. Vafapour, "Solute concentration sensing in two aqueous solution using an optical metamaterial sensor," *J. Lumin.*, vol. 230, Feb. 2021, Art. no. 117734.

[44] A. Salim and S. Lim, "Review of recent metamaterial microfluidic sensors," *Sensors*, vol. 18, no. 1, p. 232, Jan. 2018.

[45] E. S. Lari, Z. Vafapour, and H. Ghahraloud, "Optically tunable triple-band perfect absorber for nonlinear optical liquids sensing," *IEEE Sensors J.*, vol. 20, no. 17, pp. 10130–10137, Sep. 2020.

[46] Y. I. Abdulkarim, L. Deng, O. Altıntaş, E. Ünal, and M. Karaaslan, "Metamaterial absorber sensor design by incorporating swastika shaped resonator to determination of the liquid chemicals depending on electrical characteristics," *Phys. E, Low-Dimensional Syst. Nanostruct.*, vol. 114, Oct. 2019, Art. no. 113593.

[47] M. Manjappa, P. Pitchappa, N. Wang, C. Lee, and R. Singh, "Active control of resonant cloaking in a terahertz MEMS metamaterial," *Adv. Opt. Mater.*, vol. 6, no. 16, Aug. 2018, Art. no. 1800141.

[48] F. Zhou *et al.*, "Hiding a realistic object using a broadband terahertz invisibility cloak," *Sci. Rep.*, vol. 1, no. 1, pp. 1–5, Dec. 2011.

[49] H. Zou and Y. Cheng, "Design of a six-band terahertz metamaterial absorber for temperature sensing application," *Opt. Mater.*, vol. 88, pp. 674–679, Feb. 2019.

[50] Z. Vafapour, "Polarization-independent perfect optical metamaterial absorber as a glucose sensor in food industry applications," *IEEE Trans. Nanobiosci.*, vol. 18, no. 4, pp. 622–627, Oct. 2019.

[51] F. Alves, D. Grbovic, B. Kearney, N. V. Lavrik, and G. Karunasiri, "Bi-material terahertz sensors using metamaterial structures," *Opt. Exp.*, vol. 21, no. 11, pp. 13256–13271, 2013.

[52] C. Fan, Y. Tian, P. Ren, and W. Jia, "Realization of THz dualband absorber with periodic cross-shaped graphene metamaterials," *Chin. Phys. B*, vol. 28, no. 7, Jul. 2019, Art. no. 076105.

[53] O. Madelung, *Semiconductors: Group IV Elements and IIIV Compounds*. Cham, Switzerland: Springer, 1991.

[54] W. J. Ellison, "Permittivity of pure water, at standard atmospheric pressure, over the frequency range 0–25THz and the temperature range 0–100°C," *J. Phys. Chem. Reference Data*, vol. 36, no. 1, pp. 1–18, Mar. 2007.

[55] J. W. Blackett, E. C. Verna, and B. Lebwohl, "Increased prevalence of colorectal adenomas in patients with nonalcoholic fatty liver disease: A cross-sectional study," *Digestive Diseases*, vol. 38, no. 3, pp. 222–230, 2020.

[56] E. M. Stoffel and C. C. Murphy, "Epidemiology and mechanisms of the increasing incidence of colon and rectal cancers in young adults," *Gastroenterology*, vol. 158, no. 2, pp. 341–353, Jan. 2020.

[57] M. S. Cappell, "Pathophysiology, clinical presentation, and management of colon cancer," *Gastroenterol. Clinics North Amer.*, vol. 37, no. 1, pp. 1–24, Mar. 2008.

[58] J. Pan, M. Slattery, N. Shea, and F. Macrae, "Outcomes of screening and surveillance in people with two parents affected by colorectal cancers: Experiences from the familial bowel cancer service," *Hereditary Cancer Clin. Pract.*, vol. 17, no. 1, pp. 1–9, Dec. 2019.

[59] D. K. Rex *et al.*, "Colorectal cancer screening: Recommendations for physicians and patients from the US multi-society task force on colorectal cancer," *Amer. J. Gastroenterol.*, vol. 112, no. 7, p. 1016, 2017.

Zohreh Vafapour (Member, IEEE) received the B.Sc. degree in applied physics from the University of Hormozgan, Iran, in 2008, and the M.Sc. degree in condense matter physics and the Ph.D. degree in physics, optics and laser from Shiraz University, in 2011 and 2016, respectively. From July 2014 to December 2014, she was also a Visiting Ph.D. Student with the Electrical and Computer Engineering Department, The State University of New York at Buffalo, NY, USA. She has been a Postdoctoral Fellowship with Johns Hopkins University since 2016, and the Ph.D. and M.Sc. Advisor of Physics and Electrical Engineering Students. She joined the Electrical and Computer Engineering Department, and the Bio Engineering Department, University of Illinois at Chicago, in 2019. Recent years, she has hosted and participated in more than seven national and international research projects. She has authored or coauthored 27 peer-reviewed journal articles and 23 conference papers. Her research interests include optical and photonics designs/devices, plasmonics, metamaterials, optical and biomedical sensors, optical antennas, and laser cooling of semiconductors. She is an Active Member of the Optical Society of America.

William Troy received the B.Sc. degree in electrical and computer engineering from the University of Illinois at Chicago in 2018, where he is currently pursuing the Ph.D. degree in electrical and computer engineering working with the Nanoengineering Research Laboratory under Dr. Michael Stroscio. His research interests include studying and modeling laser interactions with manmade nanostructures inside of cells for remote intracellular manipulation, atomic layering of nanostructures for the creation of spontaneous polarization, non-Fourier thermodynamics, liquid condensates, and aptamer-based diagnostics for the detection of viruses and other antigens.

Ali Rashidi received the M.D. degree from the Hormozgan University of Medical Sciences, Bandar Abbas, Iran, in 2014. Since 2018, he has been working as a Postdoctoral Research Fellow with the Radiology Department, The Johns Hopkins University School of Medicine. Since 2020, he has been working as a Postdoctoral Fellowship with Stanford University. He has published seven peer-reviewed articles. His research interests include 2D and 3D MRI and metal artifact reduction sequence (MARS) MR imaging of metallic hardware, virus, and cancer detection.